

This document was produced  
by scanning the original publication.

Ce document est le produit d'une  
numérisation par balayage  
de la publication originale.

*Dr. Bowles*

**CANADA**

**DEPARTMENT OF MINES AND TECHNICAL SURVEYS**

**OTTAWA**

**MINES BRANCH INVESTIGATION REPORT IR 66-20**

**PULSE AMPLITUDE DISTRIBUTION IN  
X-RAY SPECTROGRAPHY USING  
THE SCINTILLATION COUNTER**

by

**DOROTHY J. REED**

**MINERAL SCIENCES DIVISION**

**COPY NO.**

**7**

**MARCH 29, 1966**

Mines Branch Investigation Report IR 66-20

PULSE AMPLITUDE DISTRIBUTION IN X-RAY SPECTROGRAPHY  
USING THE SCINTILLATION COUNTER

by

Dorothy J. Reed\*

- - -

SUMMARY

Pulse amplitude distribution curves have been traced for a number of elements from titanium to lead. The effect of various factors on pulse amplitude has been estimated. Escape peaks have been found for the heavier elements, and their relationship to the main peak examined.

---

\*Senior Scientific Officer, Analytical Chemistry Subdivision, Mineral Sciences Division, Mines Branch, Department of Mines and Technical Surveys, Ottawa, Canada.

## CONTENTS

	<u>Page</u>
Summary .. .. .	i
Introduction .. .. .	1
Part 1 General .. .. .	2
Abbreviations .. .. .	2
Equipment .. .. .	2
Operation of the Pulse Height Analyzer .. .. .	3
Plateaus .. .. .	3
Reproducibility .. .. .	3
Part 2 - Light Elements .. .. .	4
Pulse Amplitude .. .. .	4
Energy Resolution .. .. .	6
Amplifier Gain .. .. .	7
Conclusions .. .. .	7
Part 3 - Heavy Elements .. .. .	8
Pulse Amplitude .. .. .	8
Origin of Escape Peaks .. .. .	9
Characteristics of Escape Peaks .. .. .	10
Escape Peaks from Second and Third Order Radiation .. .. .	11
Results using Pulse Height Analyzer .. .. .	14
Conclusions .. .. .	15
References .. .. .	16
Tables 1 to 19 .. .. .	17-25
Figures 1 to 17 .. .. .	26-42

## INTRODUCTION

When the determination of hafnium in steels (1) and of lead and tantalum in ores using the K radiation of the elements was investigated, it was found that second order lines were more satisfactory than first order ones, which were masked in low concentrations by the intensity of the continuum maximum near which they occurred. Background counts were high even for second order lines so the pulse height analyzer was used to try to improve the peak-to-background ratio. Pulse amplitude distribution curves were run to determine the energy spectrum of the characteristic radiation. This was possible because the original 60V baseline of the analyzer had been extended to 150V. Once the investigation was begun, it was enlarged to include a wide range of elements and to determine the effect of various factors on pulse characteristics.

For simplicity, in this report, the elements have been divided into two groups based on the energy of their K radiation: the heavy elements which give rise to an escape peak and the light elements which do not. The heavy elements, by this definition, are those from barium to uranium, atomic numbers 56 to 92; but the spectrograph is limited by reason of critical potential to bismuth, atomic number 83 as the heaviest. The light elements are those from titanium to cesium, numbers 22 to 55. The scintillation counter is responsible for the titanium limit because it is insensitive to radiation from lighter elements.

Pulse amplitude distributions of light elements are discussed in Part 2 of this report, those for heavy elements in Part 3.

## PART 1 - GENERAL

### Abbreviations

The following abbreviations will be used in this report:

PHA	-	pulse height analyzer
PAD	-	pulse amplitude distribution
RP	-	peak of characteristic radiation, $\alpha$ or $\beta$
BP	-	peak of background radiation from the continuum
EP	-	escape peak
EP <sup>2</sup>	-	EP of an EP
A	-	pulse amplitude
W	-	width at half-height
CV	-	counter voltage
AG	-	amplifier gain
D	-	RP-EP amplitude
Z	-	atomic number

Values for  $2\theta$  and keV have been taken from ASTM tables (2).

### Equipment

A Norelco 100kV spectrograph equipped with a tungsten X-ray tube, a scintillation counter and a lithium fluorite analyzing crystal was used. The receiving collimator was four inches long with nickel plates 0.005 inches apart, while the exit collimator was one inch in length with 0.02-inch spacing. The PHA was modified making it possible to use a 60 or 150V baseline.

### Operation of the Pulse Height Analyzer

PAD curves were derived by using a channel of 0.5V to scan the characteristic radiation of an element as the baseline was varied from 60 or 150V to the beginning of noise pulses (3). Thus, only radiation within a 0.5V band was passed at any instant, though the voltage limits of this band were constantly changing. From the resulting curve which showed the intensity of the radiation with varying voltage, A and W were measured in terms of baseline voltage and W/A calculated. All peaks on a PAD curve arise from radiation reflected from a single  $2\theta$  setting, and are a measure of the various energies in this radiation.

### Plateaus

Plateaus to determine the proper operating CV were established for a number of elements at three AG settings. They are shown in Figure 1 from which plateaus for the intervening elements may be interpolated. All were determined using K $\alpha$  radiation and they show a shift to lower CV and an increase in length with increasing Z. For the individual elements there is a plateau shift to lower CV with an increase in AG.

### Reproducibility

Reported values are not absolute, but relative. Actual values may vary with a change of electronic components of the detection equipment. A change of the photomultiplier tube of the counter prior to this work caused a general plateau shift of 100V. Replacement of one of the tubes in the pulse amplifier at the conclusion of this work changed the mean of D for CV 850 from 37 to 42V.

Other factors can cause variation in results. The response of the recorder pen is slow and can make a difference in A and W of one to three volts depending on the baseline used. A and W have been estimated to the nearest 0.5V. The time required for the accumulation of these results is also a factor because the characteristics of the components may change as they age.

## PART 2 - LIGHT ELEMENTS

### Pulse Amplitude

PAD curves for K $\alpha$  radiation of a number of light elements were run with varying AG and CV. Typical curves are shown in Figure 2, which shows the effect of AG on the energy spread of FeK $\alpha$  radiation, and in Figure 3, which shows the effect of CV on SnK $\alpha$  energy. The area under the curves shows little change compared with the changes in the shape of the curves and the values of A and W. The need for the extended baseline is evident.

Values of A for several elements and the effect of AG on these values are shown in Table 1, while Table 2 shows the effect of CV within limits imposed by the plateaus. A varies directly with both AG and CV as reported by Kiley (4). From values in Table 2, the effect of CV on the relationship between keV and A was determined. Regression equations for the variation of keV with A for CV's of 800, 850, 900 and 950 at AG 10 were calculated. The slopes of these lines were 1.059, 0.668, 0.422 and 0.279

respectively. Similarly, from Table 1 the effect of AG on this relationship was calculated for CV 900. In this case the values were 0.433, 0.417, 0.351, 0.288, 0.233 and 0.190 as AG increased from 0 to 90. The slope of the lines is plotted against AG and CV in Figure 4 and shows greater change for CV.

Regressions were calculated for Ag 10 and CV 900 because in general practice these are the settings used. AG 10 keeps the noise level low, as beginning of noise in Figure 2 shows, and 900V is on the plateau of most elements.

Tables 1 and 2 also demonstrate that A varies with Z. This would be expected because A is a measure of the energy of the characteristic radiation of the elements.

Reproducibility of A and W is shown in Table 3 which presents these values for SnK $\alpha$  radiation with varying AG obtained on two clays. It may also be seen in Tables 1 and 2 by comparing values at AG 10 and CV 900.

While A varies with the conditions under which the PAD curve is obtained, the energy it measures is constant for each element. It seemed probable, therefore, that each AG, if accompanied by its mid-plateau CV, should give the same value of A and W for an element. Three PAD curves for FeK $\alpha$  radiation run at different AG's with their mid-plateau CV's are shown in Figure 5. Values from three similar PAD's for Mo and SnK $\alpha$  are listed in Table 4. Results agree within experimental limits when it is considered it is frequently difficult to determine plateau limits accurately.

### Energy Resolution

$W/A$ , expressed as percentage, is used as a measure of counter resolution (3). Smaller values for  $W$ , and hence smaller percentages, mean less spread of the energy entering the counter.  $W$  varies directly with  $A$  as the values for Fe and TiK $\alpha$  in Table 5 show.

$W/A$  for the K $\alpha$  radiation of a number of elements and the effect of AG on this ratio are shown in Table 6. Values are of the same order as those reported by Miller (3). The ratio decreases slightly with increasing AG.

The effect of CV on the spread of energy is shown in Table 7. Again the ratio decreases as the variable increases; but the decrease is more marked than that due to AG. Values at the lower end of the plateau are out of line with the rest.

The means in Table 6 show that  $W/A$  varies inversely as  $Z$ . The titanium mean is not included because a different CV was used for this element. The expected increase in  $A$  with  $Z$  has already been shown in Tables 1 and 2. The increase in  $W$  with  $Z$  is not nearly so pronounced. This results in a ratio varying inversely with  $Z$  as shown in Figure 6.  $W/A$  for strontium is out of line with the others in this figure. The large  $W$  measured for this element is reflected in a much higher ratio. Both  $A$  and  $W$  for molybdenum are low compared with those for the other elements, but the resulting ratio is of the proper magnitude.

### Amplifier Gain

On Norelco equipment the AG is continuously variable and graduated from 0 to 100. To estimate actual amplification of the pulse, from values in Table 2, the ratios of A for AG's 10 to 90 to A for AG 0 were calculated. These, with their means, are shown in Table 8 for CV 900. The last two ratios for tin and tellurium are low compared with the others. If these are omitted, the means become 2.06 and 2.67 -- not a significant change. The means are in agreement with the slopes calculated above to show the effect of AG on the relationship of keV to A. The amplitude of the incoming pulse may be continuously increased to approximately three times its original value by AG.

### Conclusions

For light elements, atomic number 22 to 56, the pulse amplitude varies directly with the atomic number of the element and with the counter voltage and amplifier gain used. The effect of applied potential is more pronounced than that of amplification.

The width of the pulse at half-height varies directly with the pulse amplitude and atomic number.

The ratio of the width of a pulse to its amplitude varies inversely with the atomic number of the element and the pulse amplitude.

### PART 3 - HEAVY ELEMENTS

#### Pulse Amplitude

As would be expected, the A values of the heavy elements exhibit the same relationship to keV as the light ones showed. This is demonstrated in Figure 7 for two CV's: the upper line at 900 and the lower at 850V. The A's for K $\alpha$  radiation of the light elements are included with those for both K $\alpha$  and R $\beta$  radiation of the heavy elements. The lines were not calculated, but have been drawn in freehand to serve as guides.

The values for the heaviest elements deviate from the lines. This may be caused by the low  $2\Theta$  angle used to obtain them. The dotted line projected from  $6^\circ 2\Theta$  emphasizes the deviation. That A's from higher  $2\Theta$  angles do not deviate as greatly is shown in Figure 8 which presents results from second and third order radiation of the heavy elements for a CV of 850. The same guide line and  $2\Theta$  projection as were used in the preceding figure are included.

Figure 7 illustrates that A's of heavy elements are affected by CV as were those of the light ones. A similar AG effect would also be expected. However, for the heavy elements, only the CV has been varied. All results have been obtained at AG 10. The high values for tellurium in Table 1 indicate that the A's of the heavy elements would soon extend beyond the 150V baseline at higher AG's.

Resolution is presented in Table 9 which may be regarded as a continuation of Table 7. It improves with increased CV as did that of the light elements. The effect of Z on resolution may be seen by comparison with Table 6. In the heavy elements it is less marked.

#### Origin of Escape Peaks

The scintillation counter consists of a thallium-activated sodium iodide crystal affixed to a photomultiplier tube. When the radiation striking the crystal has energy in excess of that of the iodine K absorption edge, iodine atoms are ionized in their K shell and the entering radiation loses the energy required for this ionization. The residual energy of the radiation appears as an EP in the PAD curve.

The keV of  $IK_{ab}$  is 33.16 (5) and all elements having characteristics energies greater than this produce an EP in addition to an RP.  $BaK\alpha$  has an energy of 32.19 and  $BaK\beta$  of 36.37 keV. Therefore, the  $\beta$  radiation will produce an EP while the  $\alpha$  will not. Their PAD curves are reproduced in Figure 9. The  $K\beta$  EP occurs at 9 baseline volts with CV 850 and partially overlaps the noise pulses. All elements heavier than barium will have an EP which will be separated from the RP by an amount on the baseline scale equivalent to 33.16 keV.

Ionization of the L shell of iodine atoms is also possible. There are three L subshells having absorption energies of 5.19, 4.86 and 4.56 keV (5). These would give a combined EP only 4.87 keV from the RP of the exciting element. In Figure 9 the overlapping barium RP's are

separated by 4.18 keV. Therefore, separation of the RP and EP in the case of iodine L ionization would not occur. The EP might be indicated by a slight broadening of the base of the RP on its low energy side.

Sodium atoms have a  $K_{ab}$  energy of only 1.08 keV so any contribution from their ionization is negligible. None of the heavy elements have L radiation of sufficient energy to produce an EP by iodine K ionization.

#### Characteristics of Escape Peaks

The A and W of an EP may be measured as are those of an RP. A values of both peaks for a number of elements at different CV's are presented in Table 10 with the resultant values for D, which should be constant at each CV and equivalent to  $IK_{ab}$  energy. S in the EP column indicates that the EP appeared as a shoulder on the RP as in Figure 10 for mercury. In general, A increases with keV for both the RP and EP of elements and with CV, though the values for HgK $\alpha$  are low. The difference in A between the  $\alpha$  and  $\beta$  radiation of an element is not so pronounced at 800V nor at higher atomic numbers.

Allowing for errors in estimating A, D is constant for each CV used. The mean value of D varies directly, but not linearly, with CV.

Reproducibility of the peaks is shown in Table 11 using WK $\alpha$  radiation from steel samples. Both first and second order radiation have been used and reproducibility is satisfactory.

From the origin of an EP, it would be expected that its W would duplicate that of the corresponding RP and that its resolution would be

poorer because its A is less. The W/A percentages for EP's shown in Table 12 prove that their resolution is poorer than that of RP's given in Table 9. The poorer resolution is due entirely to the smaller A's because W's are less than those of the corresponding RP's as Table 13 demonstrates. The ratio of the W of EP's to that of RP's is less than unity in most cases.

Each photon of radiation with sufficient energy to K ionize iodine does not produce an EP, otherwise there would be no RP. The amount of characteristic radiation represented in an EP has been evaluated by counting the squares on the chart paper under the EP and RP of a PAD curve. EP's, as a percentage of the sum, are contained in Table 14 for first and second order radiation. From this rough determination there would seem to be no correlation with keV or CV. The mean of the first order estimates is 15, that of the second order 24%.

#### Escape Peaks From Second and Third Order Radiation

For heavy elements with small  $2\Theta$  angles for their characteristic radiation, second or third order radiation gave better A values than first order did. This fact led to an investigation of the effect of higher order radiation on EP characteristics.

When first order radiation is used, the continuum background has the same energy as the radiation and the BP coincides with the RP. When second or third order radiation is employed, this is not the case. Then the background is of lower energy, and the BP is separated from the RP. Table 15 lists  $2\Theta$  angles for first, second and third order radiation of a

number of heavy elements with the keV of the radiation in the case of the first order, but of the background for the other orders. The energy of any resulting EP's is also listed, except those possible from first order EP's of the heaviest elements or EP<sup>2</sup>'s.

Considering barium for second order K $\alpha$  radiation, there would be an RP and a BP at approximately half the A of the RP. For K $\beta$  radiation, there would be an EP in addition. These curves are shown in Figure 11 with the K $\beta$  RP at 71, its BP at 36.5 and its EP at 14 V using CV 900.

The light elements also give a BP with higher orders of radiation as is shown for second order SnK $\alpha$  in Figure 12. Inexperience might cause this BP to be mistaken for an EP or for an RP of another element, in which case the tin would be judged impure.

With the heavy elements, as Z increases the situation arises where the BP has energy approaching that of the EP and the two peaks cannot be resolved. This is illustrated by first and second order HfK $\alpha$  in Figure 13 where the BP has increased the size of the EP in the second order curve. Such peak coincidence could cause a spurious estimate of the energy in the EP and is responsible for the high second order percentages in Table 14. This discrepancy in energy estimation is magnified if varying concentrations of an element are compared. The results in Table 16 for tungsten in steel confirm this. As the amount of tungsten decreased, the BP approached equivalence with the RP and, coinciding with the EP, greatly increased the apparent energy in the latter. For first order results, the energy in the EP was constant regardless of the concentration.

At still larger values of Z, background and EP energies again diverge while both have sufficient energy to cause EP's of their own. Figure 14 exhibits two PAD curves for second order  $\text{PbK}\beta_1$ . Each curve has three peaks with the RP's occurring at 83 and 49 baseline volts. From Table 10, for an RP of 83V at CV 850 an EP of 46V would be expected. Similarly, an EP of 27V would be expected for an RP of 49V at CV 800. Both EP's are higher than expected, occurring at 52 and 31V respectively. However, if energies alone are considered, then 84.91 keV of the RP occur at 83V and 51.75 keV of the EP at 52V. Hence, the BP (42.33 keV) should occur at approximately 42V, the background EP at 9V and the  $\text{EP}^2$  at 18.5V. The continuum from lead is much smaller than that from many lighter elements because of the high absorption of X-rays by the metal. Any BP from it at 42V would be insignificant compared with the EP at 52V. Thus, the three peaks of the 850V PAD are the RP, EP and  $\text{EP}^2$  of  $\text{PbK}\beta$  ( $n=2$ ). Substitution of CV 800 voltages results in the same conclusion regarding the peaks of the second curve.

Figure 15 shows curves for third order  $\text{HgK}\alpha$ . In this instance, the RP and BP occur as expected, but the EP is displaced from the expected 42 to 54V. There is no ready explanation for the EP displacement but it is confirmed by Figure 16 where the EP of third order  $\text{HfK}\beta$  is displaced to become a shoulder on the RP.

In many cases it is not possible to measure W of EP's from second order radiation, but A can usually be estimated. Values of A for RP and EP from second order  $\alpha$  and  $\beta$  radiation and the resulting D's are

given in Table 17. Though its spread is greater, the mean values of D agree well with those for first order in Table 10.

#### Results Using Pulse Height Analysis

The effect of PHA settings on the regression characteristics of standards for the determination of hafnium in steels (6) is shown in Table 18 which lists the standard error and the covariance of the mean percentage of hafnium determined ( $\bar{y}$ ) for three thresholds. For the 6V threshold, which eliminated only the noise, and the 39V one, which eliminated all energy below the EP, these values are of the same order. For the highest threshold, which counted only the RP and higher energies, both figures improved significantly. This improvement was reflected in the background counts. With a 6V threshold, the mean background was 3061 cps with a standard deviation of  $\pm 22$ . With a 39V threshold these values became 2931 cps and  $\pm 19$ , while for 75V they decreased to 1288 cps and  $\pm 11$ .

For the determination of hafnium in niobium, the PHA again proved effective. Five synthetic powdered standards, prepared by dissolving hafnium and niobium in hydrofluoric and nitric acids, taking the solutions to dryness and powdering the residues, were counted in duplicate at HfK $\alpha$  ( $n=2$ ) with the background measured at  $15^\circ 2\theta$  LiF. Counts were made using 80 kV, 20 mA, AG 10 and CV 900. Three PHA settings were used: a 6V threshold and infinite channel to eliminate the noise, a 45V threshold and 30V channel to pass only the EP energy and a 75V threshold with a 60V channel to count the RP only. The characteristics of the resulting regression lines are shown in Table 19. Both total and net counts were used. All gave

the same results within the limits of error of the methods. For this determination background counts are unnecessary. The contribution of the background is shown by the values of the intercept "a" and the counts obtained from the blank. The sensitivity is of the same order whether the total radiation or only the RP is used as slope "b" shows, but the use of the RP alone decreases the error. The use of the EP decreases the sensitivity as would be expected. It is decreased by a factor of six while the error is doubled.

Figure 17 reproduces scans of NBS steel standard 841 made over second and third order WK peaks with different PHA settings. When the PHA is set to pass K $\beta$ EP pulses only, the K $\beta$ RP is almost eliminated and the K $\alpha$  greatly reduced. RP settings have no effect on the tungsten peaks. The combination curve is the sum of the other two. For analytical purposes, the RP curve gives a better signal-to-noise ratio for second order radiation. The combined curve gives greater sensitivity for third order energy.

### Conclusions

For heavy elements the amplitude of the radiation peak varies directly with the keV of the radiation until  $2\theta$  angle approaches  $5^\circ$ .

For elements having  $2\theta$  less than  $6^\circ$  for first order radiation, the second or third order gives better values for the amplitude of the radiation peak.

The amplitude of the escape peak also varies directly with the keV of the characteristic radiation.

Escape peaks from second order radiation must be carefully interpreted because background radiation may have similar energy and thus affect the escape peaks' width at half-height and the apparent amount of energy they contain.

Escape peaks from third order radiation do not occur at the expected amplitude.

Escape peaks contain approximately 15% of the energy in the first order characteristic radiation.

The difference between the amplitudes of the radiation and escape peaks is constant for each counter voltage if the amplifier gain is unchanged.

#### REFERENCES

1. D. J. Reed - "The Determination of Small Amounts of Hafnium in Mild Steels by X-ray Spectrography", Mines Branch Investigation Report IR 65-23 (March 18, 1965).
2. ASTM Data Series DS 37 - "X-ray Emission Line Wavelength and Two Theta Tables" (July 1965).
3. D. C. Miller - "Some Considerations in the Use of Pulse Height Analysis with X-rays", Norelco Rptr. 4, 37 (1957).
4. W. R. Kiley - "The Functions and Application of Counters and the Pulse Height Analyzer", Norelco Rptr. 7, 143 (1960).
5. S. Fine and G. F. Hendee - "A Table of X-ray K and L Emission and Critical Absorption Energies for all Elements", Norelco Rptr. 3, 113 (1965).
6. D. J. Reed - "The Determination of Zirconium, Niobium and Hafnium in Low Alloy Steels by X-ray Spectrography", Mines Branch Research Report R174 (1966).

TABLE 1

Effect of Amplifier on Pulse Amplitude

AG	A at CV 900						
	Fe	Zn	Se	Sr	Mo	Sn	Te
0	11	14.5	21.5	29	32	55	58
10	11.5	15	22.5	30	33	57	60.5
30	14	18	27	36	40	67.5	72.5
50	17.5	23	34	45	49.5	84	88.5
70	23	30	44	58.5	72	105	111
90	30	39	56	76	94	131.5	136.5

TABLE 2

Effect of Counter Voltage on Pulse Amplitude

CV	A at AG 10							
	Ti	Fe	Zn	Se	Sr	Mo	Sn	Te
700							8	8
750						7.5	13	14
800				8	11.5	12.5	22	22.5
850			9.5	14	19.5	21	34.5	37.5
900		11.5	15	22.5	31.5	33	57	59.5
950	12.5	17.5	24.5	36	48.5	53	86	94
keV	4.51	6.40	8.64	11.22	14.16	17.48	25.27	27.47

TABLE 3

Replication of Measurements

AG	A for SnK $\alpha$ at CV 900			
	First Day		Second Day	
	A	W	A	W
0	55	16	52.5	16
10	57	16.5	54.5	16
30	67.5	19	66	19.5
50	84	23	81	22.5
70	105	26	100.5	26
90	130.5	28	126	27

TABLE 4

A and W using CV at Mid-plateau

AG	SnKa			MoKa		
	CV	A	W	CV	A	W
10	840	32	10.5	860	26	10.5
50	790	28	10	810	24	10
90	740	28.5	10	750	22	9

TABLE 5

A and W of Fe and Ti at CV of 950

AG	FeKa		TiKa	
	A	W	A	W
10	17.5	11	12.5	8.5
30	21	12.5	15.5	10
70	33.5	20	25	16

TABLE 6

Effect of Amplifier on Energy Resolution

Element	Z	CV	Resolution: W/A						Mean
			AG 0	AG 10	AG 30	AG 50	AG 70	AG 90	
Ti	22	950		68	65		64		
Fe	26	900	64	65	61	63	63	62	63
Zn	30	900	55	53	54	52	53	49	53
Se	34	900	44	44	44	44	43	41	43
Sr	38	900	48	46	42	40	38	36	42
Mo	42	900	36	35	35	34	33	32	34
Sn	50	900	29	29	28	27	25	21	27
Te	52	900	28	28	27	27	24	20	26

TABLE 7

Effect of CV on Energy Resolution

Element	Resolution at AG 10					
	CV 700	CV 750	CV 800	CV 850	CV 900	CV 950
Fe				73	67	63
Zn				56	53	52
Se			50	46	44	43
Sr			56	46	44	37
Mo		47	40	36	35	34
Sn	75	50	36	32	29	27
Te	88	54	40	30	28	27

TABLE 8

Effect of Amplifier on A Ratios

AG	Ratio of A to A at AG 0 with CV 900							
	Fe	Zn	Se	Sr	Mo	Sn	Te	Mean
0	1.00	1.00	1.00	1.00	1.00	1.00	1.00	1.00
10	1.04	1.02	1.05	1.03	1.03	1.04	1.04	1.03
30	1.25	1.24	1.26	1.24	1.26	1.25	1.25	1.24
50	1.58	1.56	1.58	1.55	1.55	1.54	1.52	1.55
70	2.09	2.04	2.05	2.02	2.09	1.91	1.91	2.02
90	2.72	2.67	2.60	2.62	2.76	2.39	2.35	2.59

TABLE 9

Effect of CV on Energy Resolution

Element	Resolution at AG 10							
	800V		850V		900V		950V	
	K $\alpha$	K $\beta$	K $\alpha$	K $\beta$	K $\alpha$	K $\beta$	K $\alpha$	K $\beta$
Ba 56				27		24		
Ce 58			30	26	25	22	24	20
Nd 60			26	25	23	23	21	18
Gd 64	24	28	23	23	23	21	17	
Er 68	25	30	23	29	21	23		
Hf 72	24	34	22		20	29		
Ta 73	26	31	23	30	21	28		
W 74	27	34	25		19	25		
Pt 78	32	31	28	29				
Hg 80	31	32	28	30				
Pb 82		35		37		31		

TABLE 10

Amplitudes of Radiation and Escape Peaks of Various Elements

n=1	800V			850V			900V			950V		
Radiation	RP	EP	D	RP	EP	D	RP	EP	D	RP	EP	D
Ba K $\beta$				47.5	9	38.5	71	14	57			
Ce K $\alpha$				44	6	38	67	10	57	105	16	89
K $\beta$				51	13	38	77	20	57	119	32	87
Nd K $\alpha$				49	10	39	73	15.5	57.5	113	25	88
K $\beta$				55	17	38	83	26	57	127	42	85
Gd K $\alpha$	37	15.5	21.5	55.5	17	38.5	80	25	55	142	62	80
K $\beta$	38	15	23	60	23	37	99	40.5	58.5			
Er K $\alpha$	36	14.5	21.5	61	25	36	97	39.5	57.5			
K $\beta$	39.5	19	20.5	67	31.5	35.5	104.5	50	54.5			
Hf K $\alpha$	40	19	21	68	33	35	103	50	53			
K $\beta$	41	19	22	70.5	36	34.5	112	56	56			
Ta K $\alpha$	46	23	23	74	37	37	115	58	57			
K $\beta$	46.5	23.5	23	76	38	38	118.5	60	58.5			
W K $\alpha$	48	24	24	76.5	38.5	38	124	64	60			
K $\beta$	49.5	26	23.5				126	S				
Pt K $\alpha$	50	29	21	83	46	37						
K $\beta$	51	28	23	83	46	37						
Hg K $\alpha$	49	S		81	S							
Mean			22			37			57			86

TABLE 11

Reproducibility of Measurements - Tungsten in Steel

% W	Ka Peak	750V			800V			850V			900V		
		RP	EP	D	RP	EP	D	RP	EP	D	RP	EP	D
18.5	n=1	28.5	15	13.5	48	24	24	79	40.5	38.5	122	64.5	57.5
18.5	n=2	29	14.5	14.5	45.5	23	22.5	75.5	38.5	37	118	61.5	56.5
13.0	n=2	29	15	14	49	25	24	80.5	41	39.5	124	65	59
7.8	n=1										124.5	66	58.5
7.8	n=2	29.5	15.5	14									
2.8	n=2	29.5	15.5	14	49	25	24	79.5	41	38.5	123	64	59

TABLE 12

Resolution of Energy in Escape Peaks

Element	Resolution							
	800V		850V		900V		950V	
	Ka	Kβ	Ka	Kβ	Ka	Kβ	Ka	Kβ
Ce			66	76	90	60	81	51
Nd			100	59	77	50	66	48
Gd	48	50	61	46	42	37	36	
Er	52	55	44	42	43	33		
Hf	43	30	39		35	53		
Ta	43	57	38	55	38	45		
W	44		39		30			

TABLE 13

Ratio of W of Escape Peak to that of Radiation Peak

Element	800V		850V		900V		950V	
	K $\alpha$	K $\beta$	K $\alpha$	K $\beta$	K $\alpha$	K $\beta$	K $\alpha$	K $\beta$
Ba				0.62		0.65		
Ce			0.67	0.74	0.54	0.71	0.52	0.68
Nd			0.77	0.74	0.71	0.68	0.61	0.87
Gd			0.88	0.75	0.83	0.71	0.83	0.71
Er	0.83	0.87	0.78	0.69	0.85	0.69		
Hf	0.85	1.00	0.82		0.82	1.00		
Ta	0.83	0.93	0.82	0.91	0.92	0.82		
W	0.81		0.79		0.79			

TABLE 14

Energy in Escape Peaks

Radiation	First Order				Second Order		
	800V	850V	900V	950V	800V	850V	900V
Ba K $\beta$		22	10				11
Ce K $\alpha$			22	19			
K $\beta$		18	21	19			
Nd K $\beta$		17	20	16			
Gd K $\alpha$		16	13	24			
K $\beta$		12	14	16			
Er K $\alpha$	19	16	16				
K $\beta$	16	17					
Hf K $\alpha$	11	13	11		21		21
K $\beta$	12		12				30
Ta K $\alpha$	13	11	11		24	21	21
K $\beta$	12	13			25	25	25
W K $\alpha$	14	12			21	21	21
K $\beta$					23	21	21
Pt K $\alpha$					21	21	20
K $\beta$					30	28	23
Hg K $\alpha$					25	26	
K $\beta$					34	37	

TABLE 15

Characteristic Radiation and Background Energies

		First Order			Second Order			Third Order	
		2 $\theta$ LiF	keV	EP	2 $\theta$ LiF	bg keV	bg EP	2 $\theta$ LiF	bg keV
Ba	K $\alpha$	10.97	32.19		22.05	16.10		33.34	10.73
	K $\beta$	9.71	36.37	3.21	19.49	18.18		29.41	12.13
Ce	K $\alpha$	10.18	34.71	1.55	20.43	17.36		30.86	11.57
	K $\beta$	9.00	39.25	6.09	18.05	19.62		27.22	13.08
Nd	K $\alpha$	9.45	37.35	4.19	18.97	18.67		28.63	12.45
	K $\beta$	8.35	42.27	9.11	16.75	21.13		25.24	14.09
Gd	K $\alpha$	8.21	42.98	9.82	16.47	21.48		24.81	14.33
	K $\beta$	7.24	48.72	15.56	14.52	24.34		21.85	16.24
Er	K $\alpha$	7.19	49.09	15.93	14.41	24.52		21.68	16.38
	K $\beta$	6.34	55.68	22.52	12.70	27.66		19.09	18.56
Hf	K $\alpha$	6.32	55.80	22.64	12.67	27.92		19.05	18.60
	K $\beta$	5.57	63.38	30.22	11.15	31.70		16.76	21.12
Ta	K $\alpha$	6.13	57.54	24.36	12.28	28.75		18.48	19.18
	K $\beta$	5.41	65.21	32.05	10.83	32.75		16.28	21.74
W	K $\alpha$	5.95	59.30	26.41	11.92	29.66		17.92	19.76
	K $\beta$	5.25	67.23	34.07	10.51	33.63	0.47	15.79	22.38
Pt	K $\alpha$	5.28	66.83	33.67	10.57	33.43	0.27	15.88	22.28
	K $\beta$	4.66	75.76	42.60	9.32	38.00	4.84	14.00	25.26
Hg	K $\alpha$	4.98	70.79	37.63	9.98	35.37	2.21	14.99	23.60
	K $\beta$	4.40	80.23	47.07	8.80	40.13	6.97	13.22	26.74
Pb	K $\alpha$	4.71	74.98	41.82	9.42	37.45	4.29	14.15	25.01
	K $\beta$	4.16	84.91	51.75	8.32	42.33	9.17	12.49	28.31

TABLE 16

Energy in Escape Peaks - Tungsten in Steels

% W	Energy in K $\alpha$ EP	
	n = 1	n = 2
18.5	10	24
13.0		27
9.7	10	30
5.7		38
1.7	10	49
0	10	66

TABLE 17

Radiation and Escape Peaks of Second Order Radiation of Elements

Radiation	750V			800V			850V			900V		
	RP	EP	D	RP	EP	D	RP	EP	D	RP	EP	D
Nd Ka							47	10.5	36.5			
K $\beta$							54.5	17.5	37			
Gd Ka							55	19	36			
K $\beta$							62	30.5	31.5			
Er Ka							60	30	30	94	46.5	47.5
K $\beta$				41	21	20	67	34.5	32.5			
Hf Ka				40	19.5	20.5	68	36.5	37.5	102	51	51
K $\beta$				44	18	26	75.5	43.5	38.5	112.5	60	52.5
Ta Ka				46	23	23	74	37.5	36.5	115.5	60	55.5
K $\beta$				49	25.5	23.5	81.5	43.5	38	127	69	58
W Ka	28.5	15	13.5	47	23.5	23.5	77	39.5	37.5			
K $\beta$	29	15.5	13.5	55.5	29	26.5	85.5	45.5	40	136	75.5	60.5
Pt Ka				55	28.5	26.5	86	46	40	134	73.5	60.5
K $\beta$				57	31.5	25.5	90	50	40	141	81	60
Hg Ka	33	17.5	15.5	55.5	28.5	27	88.5	46	42.5	136.5	73.5	63
Mean			14			24			37			56.5

TABLE 18

Hafnium in Steels - Regression Characteristics for Second Order Ka Radiation

Threshold	Energy Passed	Error	CV of $\bar{y}$
6V	all - noise	$\pm 0.013$	$\pm 11.06\%$
39V	EP + RP	$\pm 0.014$	$\pm 11.91\%$
75V	RP only	$\pm 0.006$	$\pm 5.11\%$

TABLE 19

Hafnium in Niobium - Regression Characteristics for Second Order  
K $\alpha$  Radiation

Method	a	b	Correlation Coefficient	Error	0% Hf cps	
					calc.	obs.
EP net	-3.31	0.052676	+0.9974	$\pm 0.55$	63	65
EP total	-35.59	0.043791	+0.9974	$\pm 0.54$	813	828
RP net	-0.19	0.007694	+0.9995	$\pm 0.24$	25	20
RP total	-1.78	0.007208	+0.9995	$\pm 0.24$	245	245
6V net	-0.015	0.007397	+0.9987	$\pm 0.39$	20	20
6V total	-8.46	0.006911	+0.9990	$\pm 0.32$	1224	1252

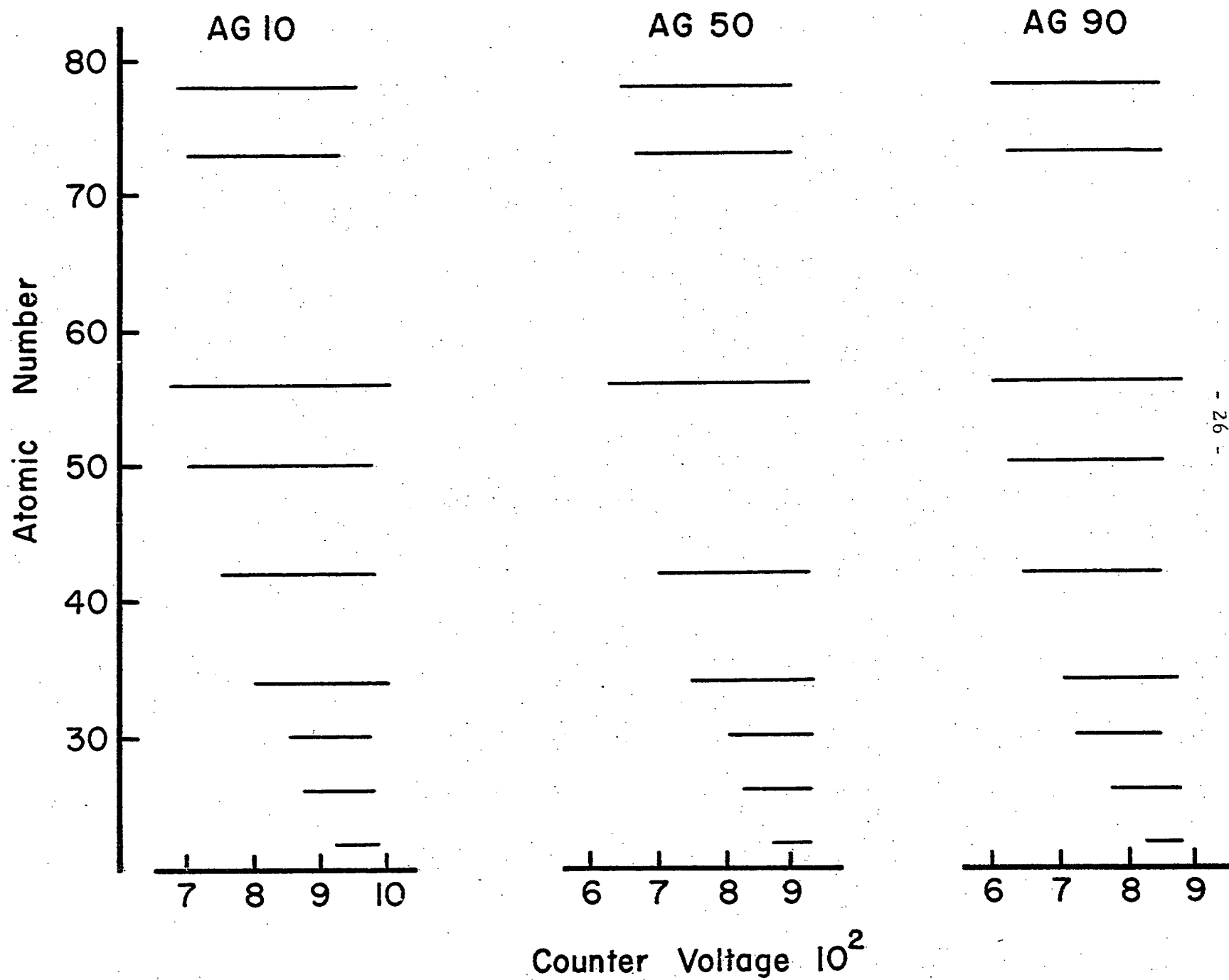


Figure 1. Scintillation Counter Plateaus for Various Elements.

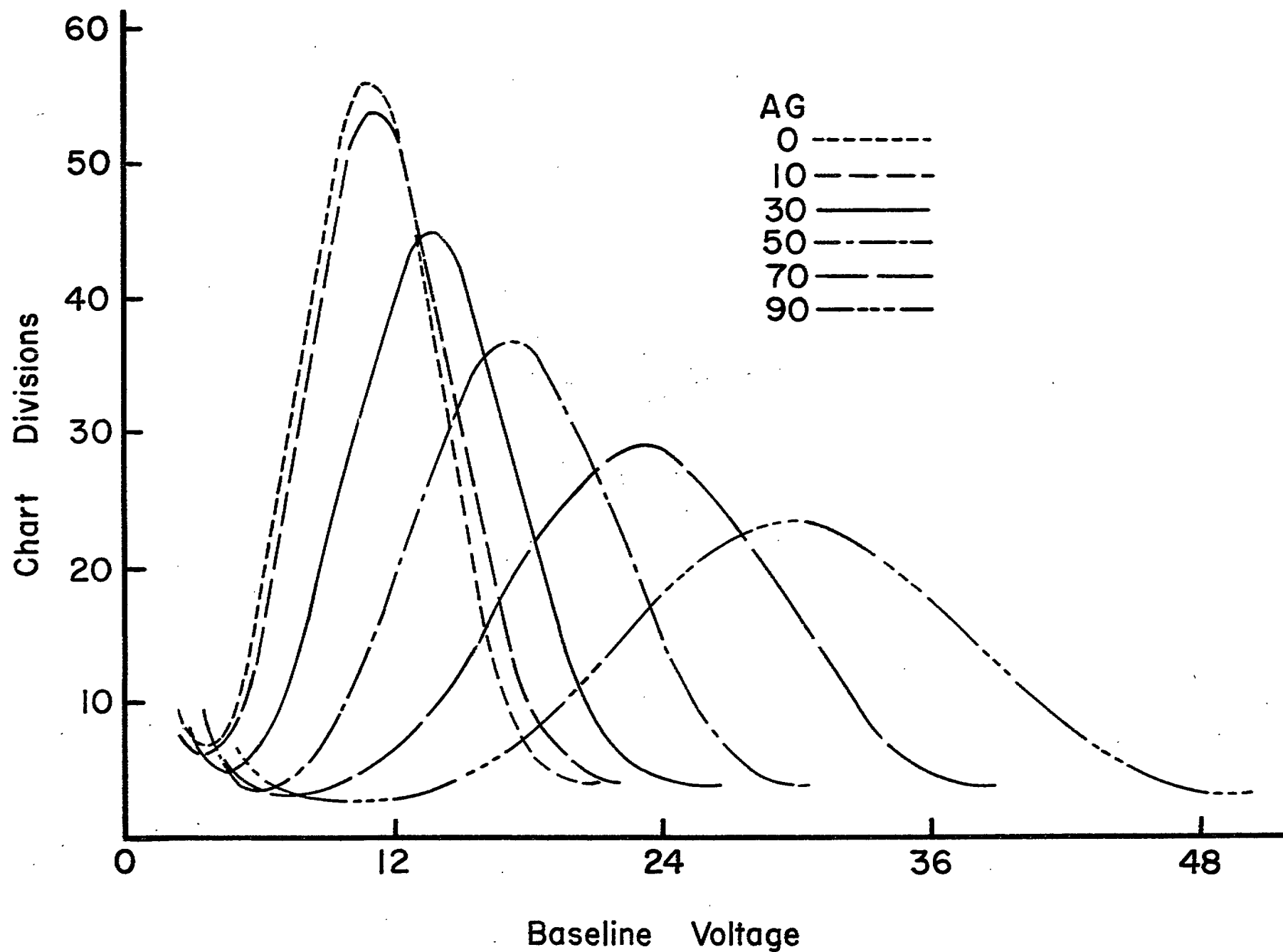


Figure 2. Effect of Amplifier Gain on FeKa Pulse Amplitude.

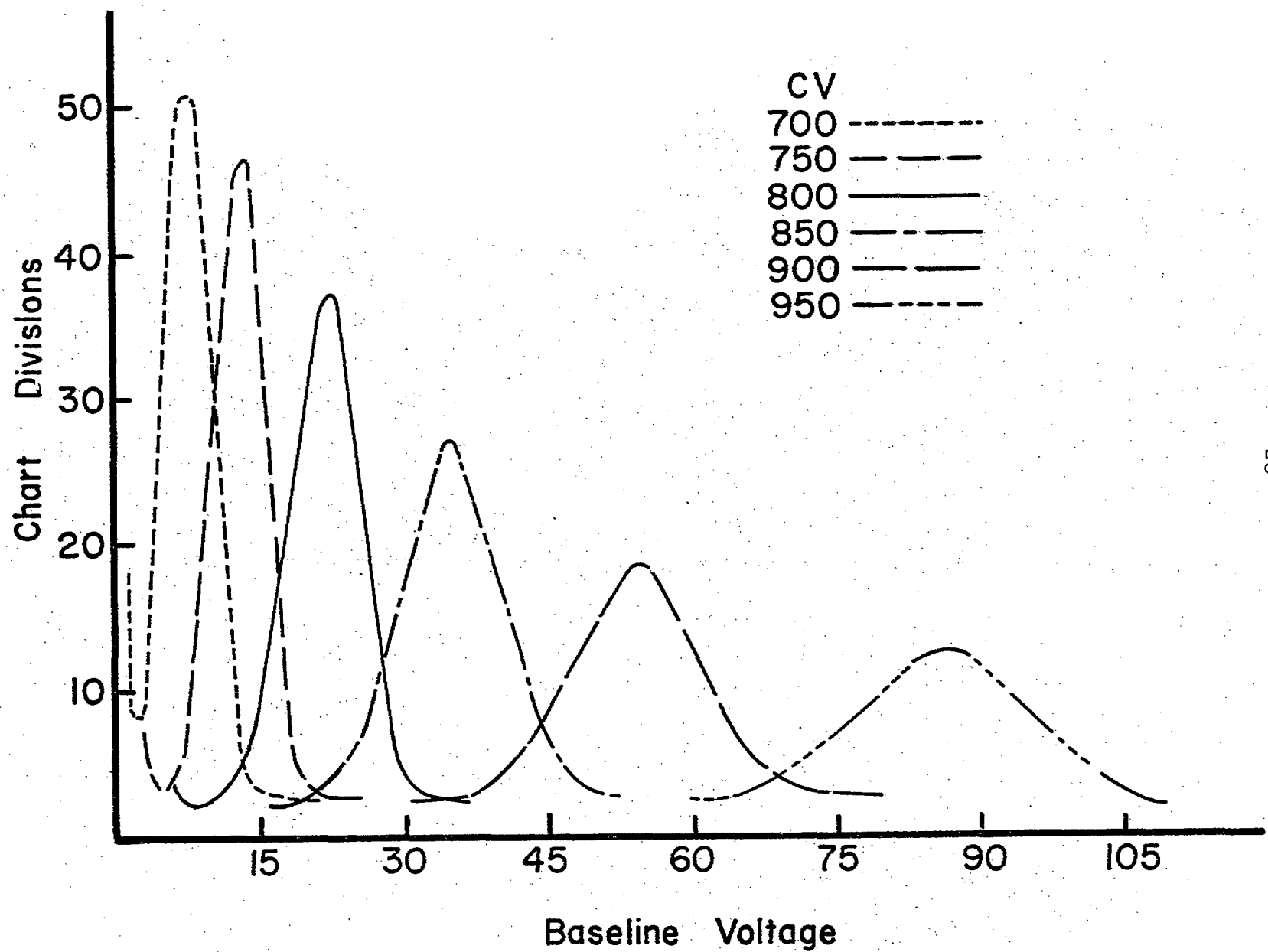


Figure 3.. Effect of Counter Voltage on SnKa Pulse Amplitude.

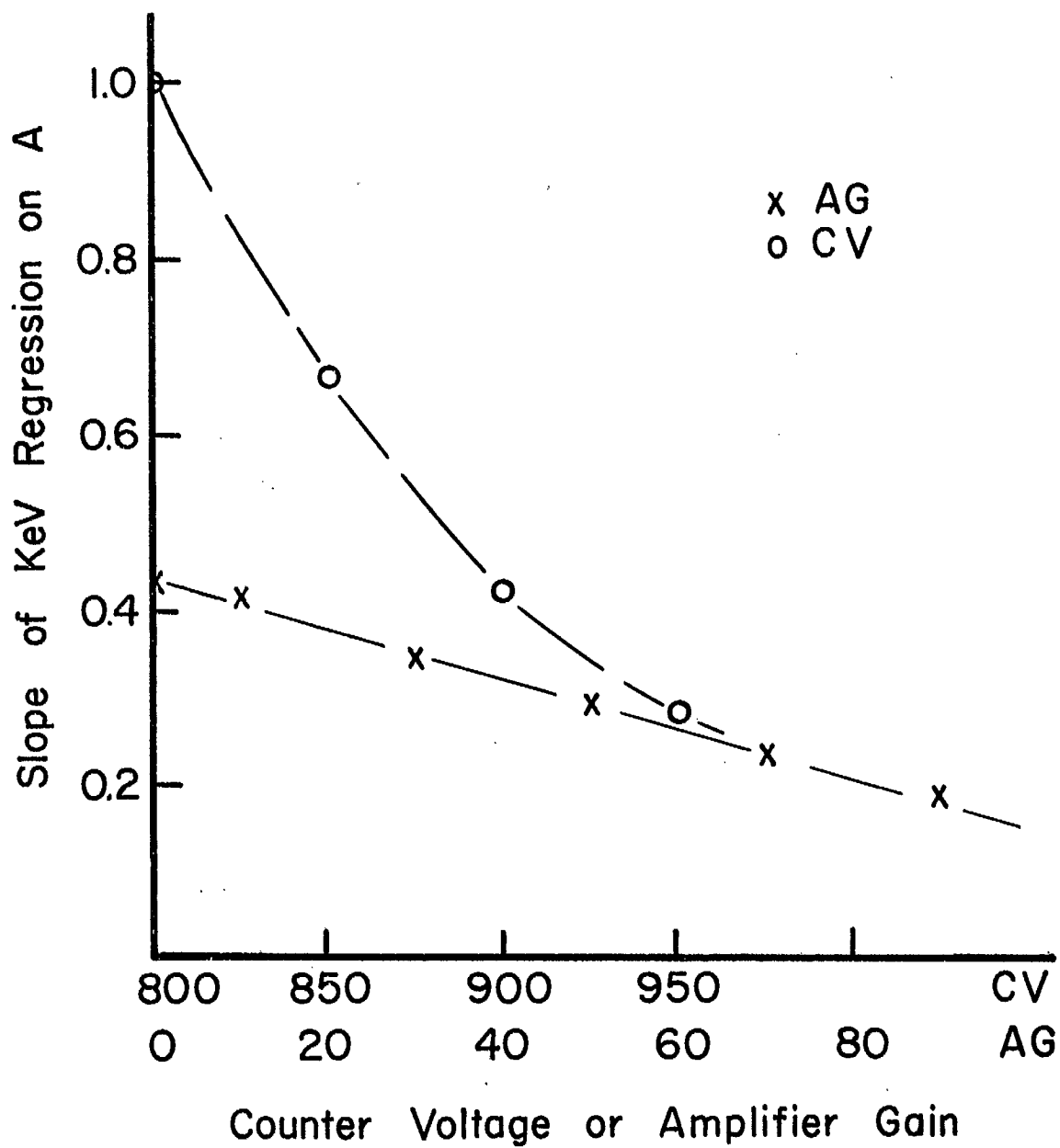


Figure 4. Effect of Counter Voltage and Amplifier Gain on Regression of keV on A.

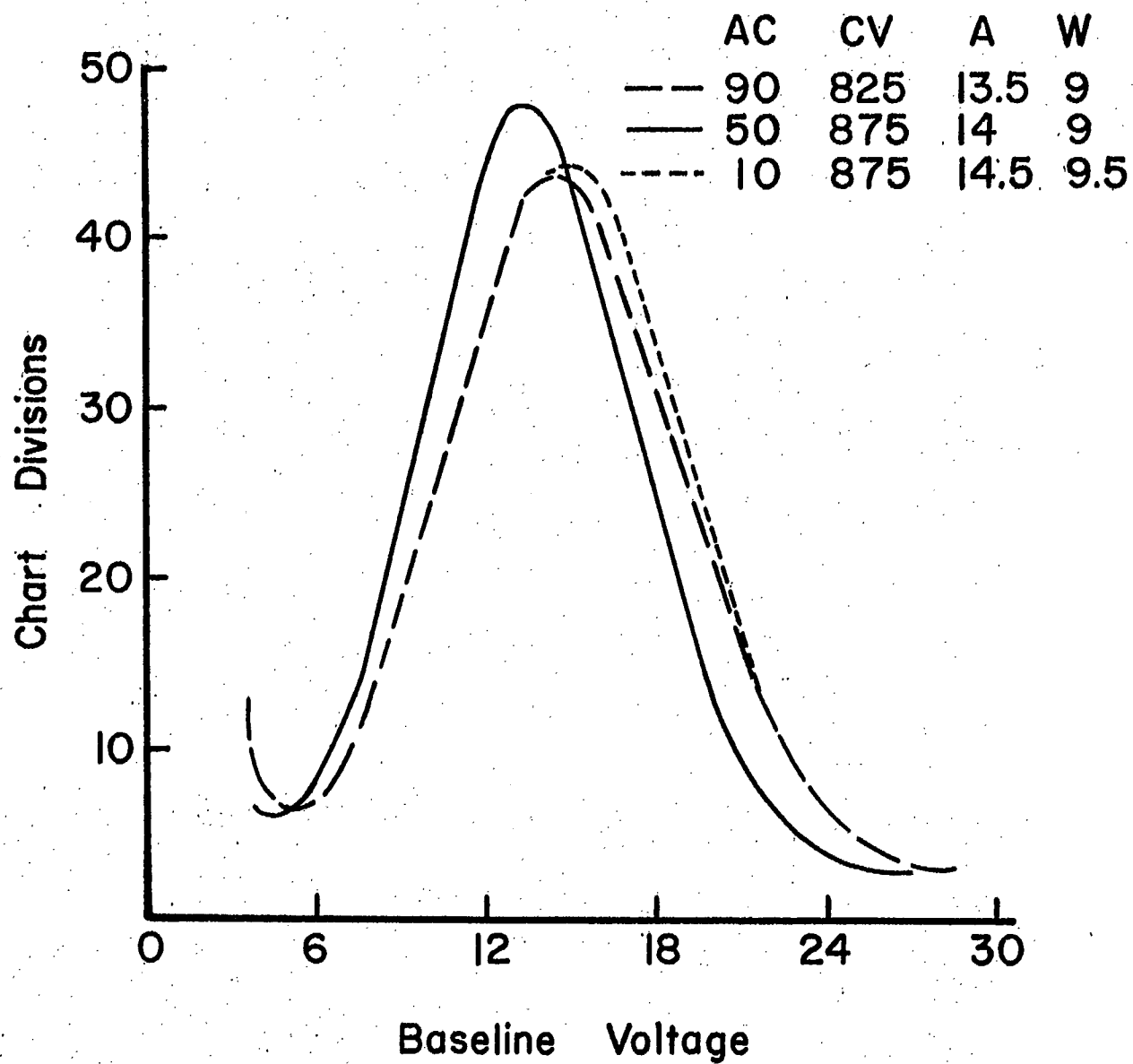


Figure 5. FeKa PAD Curves Using Mid-plateau CV with Different AG's.

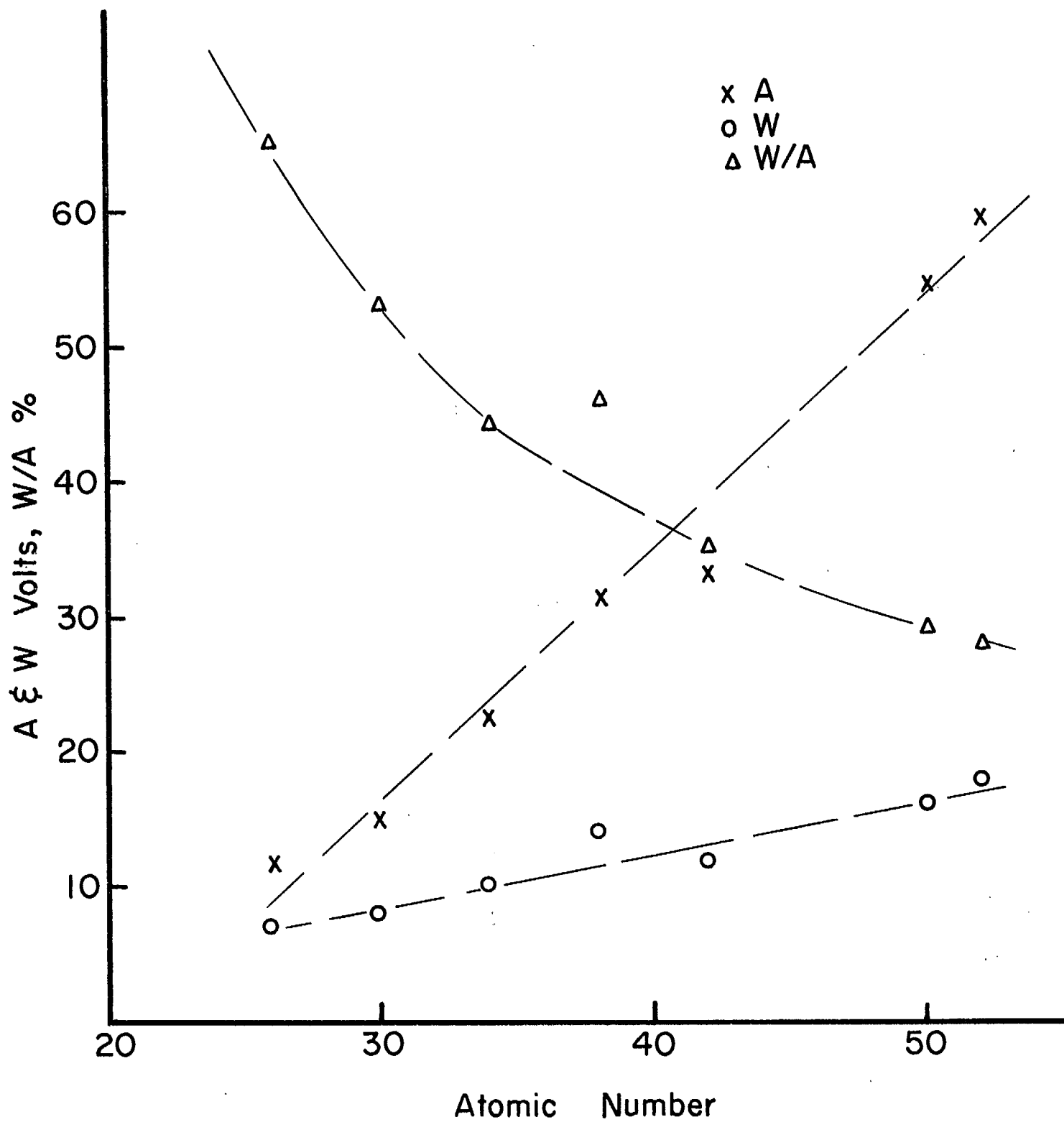


Figure 6. Effect of Atomic Number on Pulse Characteristics.

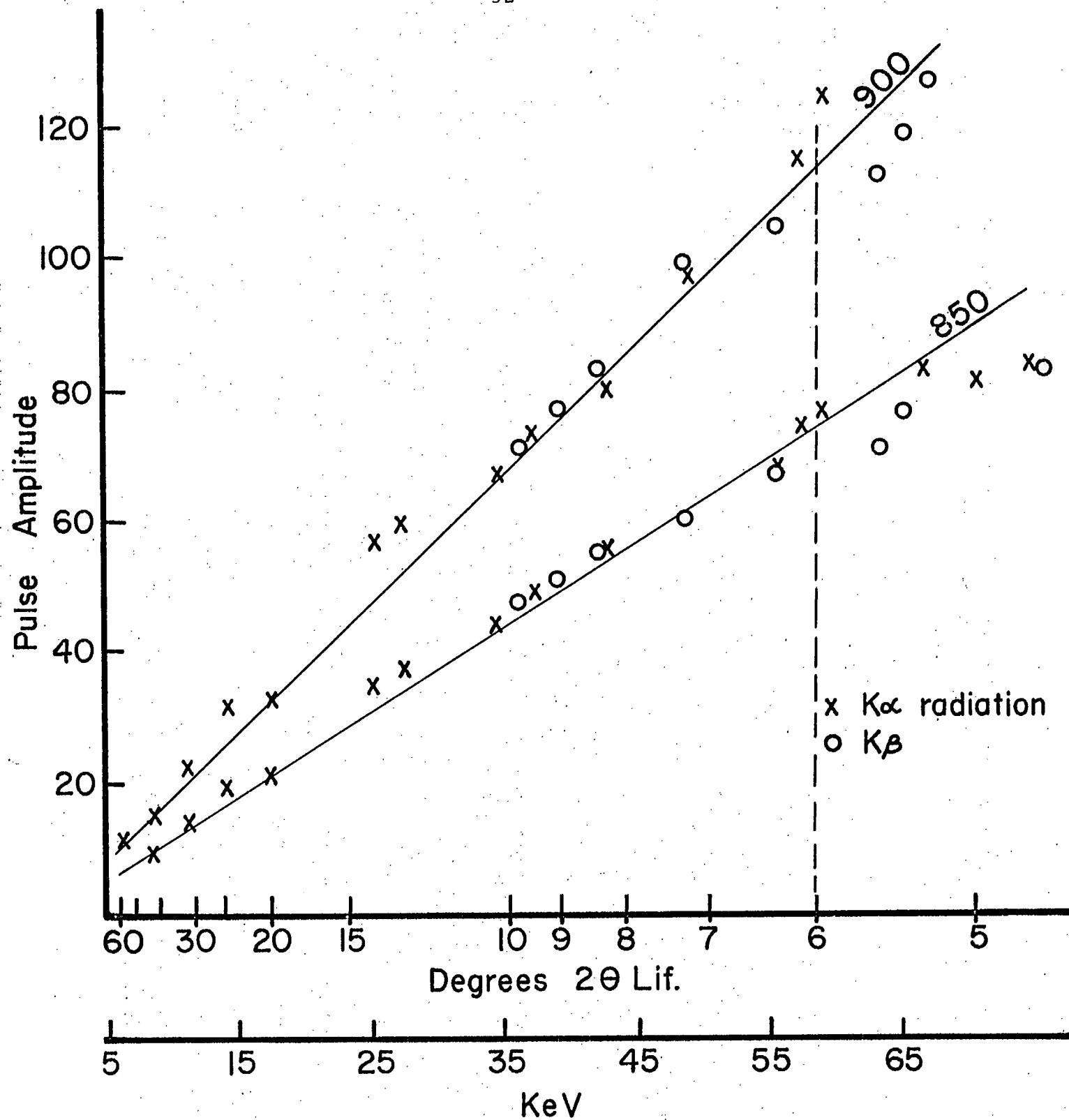


Figure 7. Variation in A with keV for CV 850 and 900.

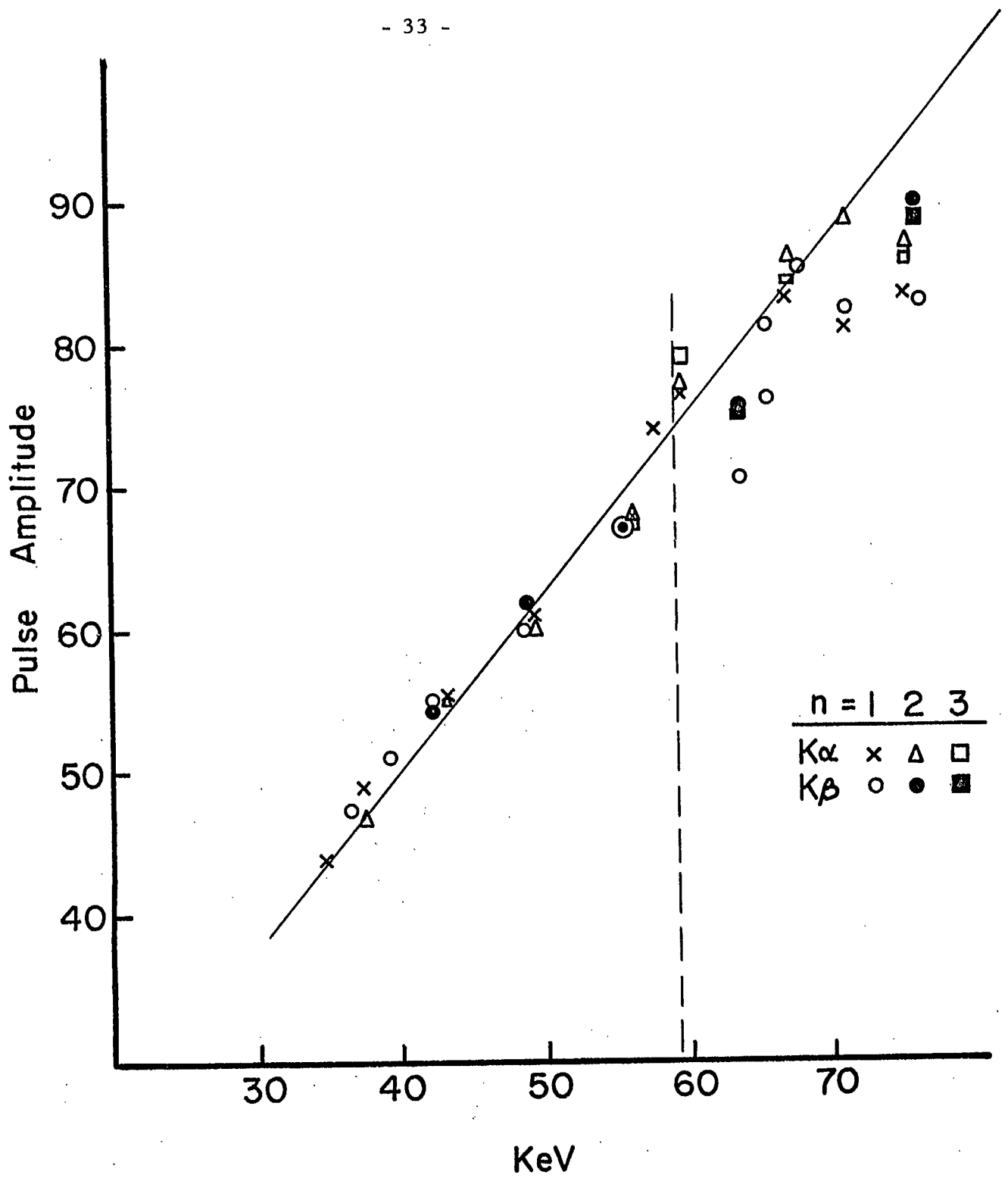


Figure 8. Variation in A with keV for Different Orders of Radiation of CV 850.

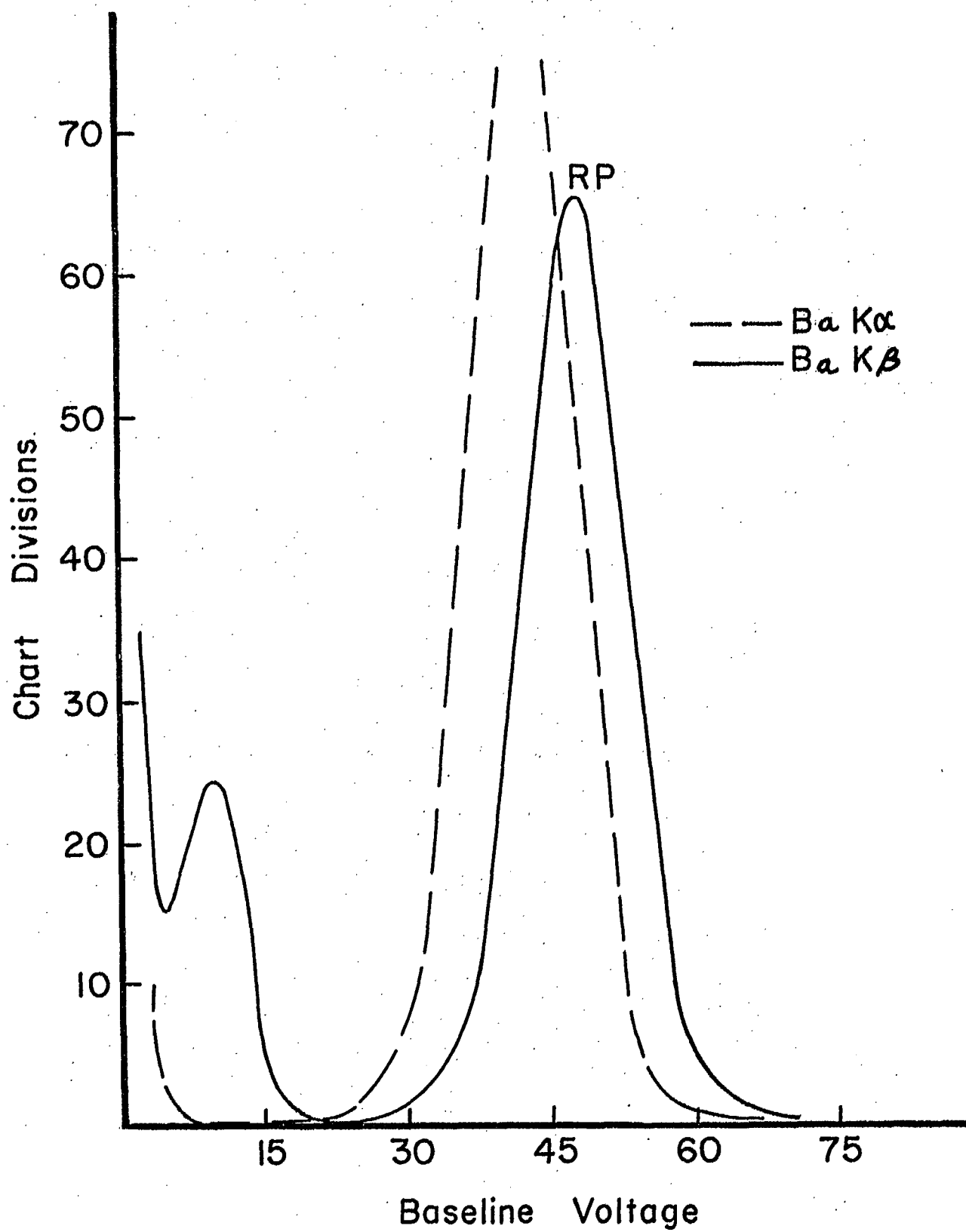


Figure 9. PAD Curves for First Order Barium Radiation at AG 10 and CV 850.

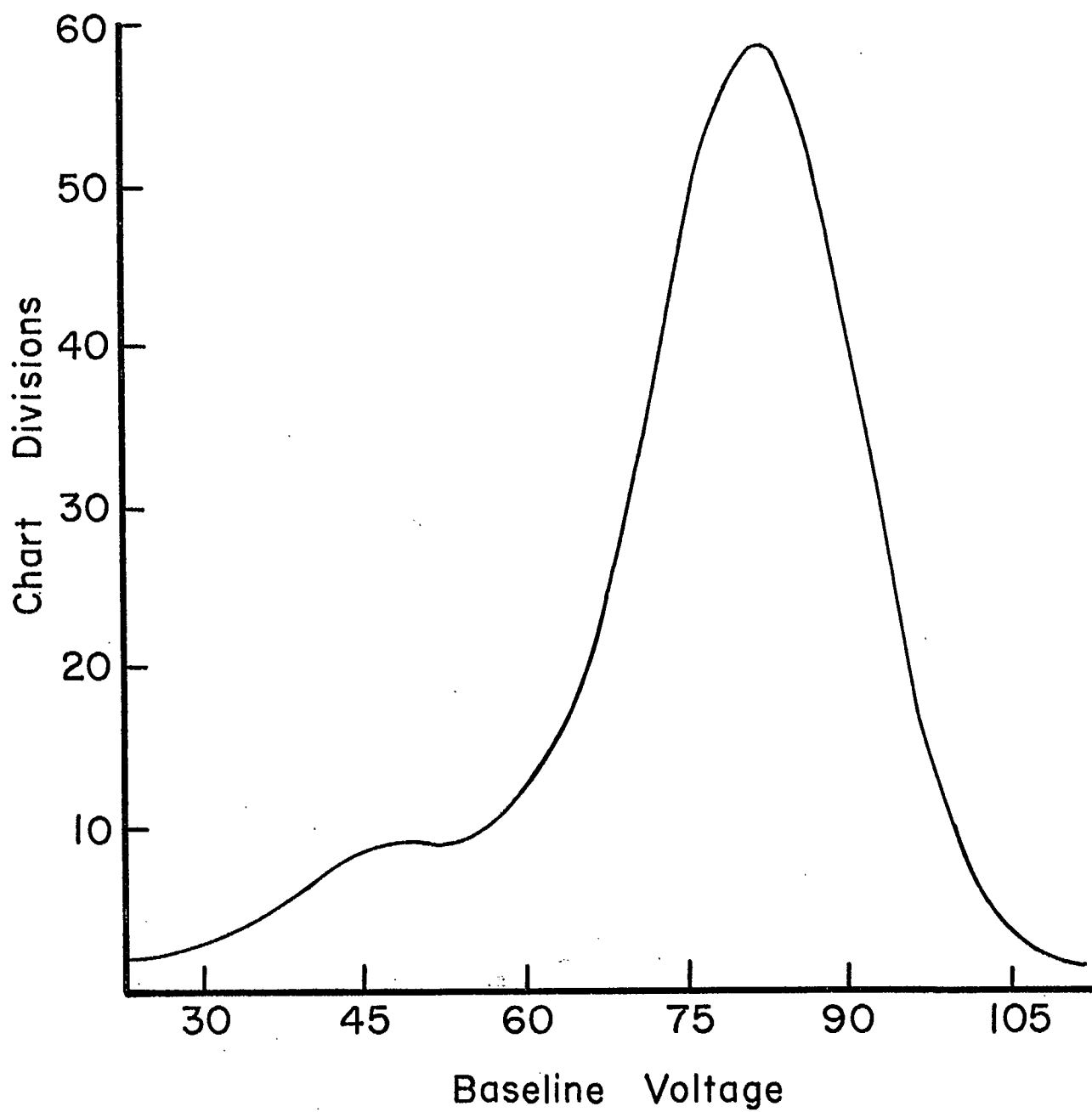


Figure 10. HgKa PAD Curves at CV 850.

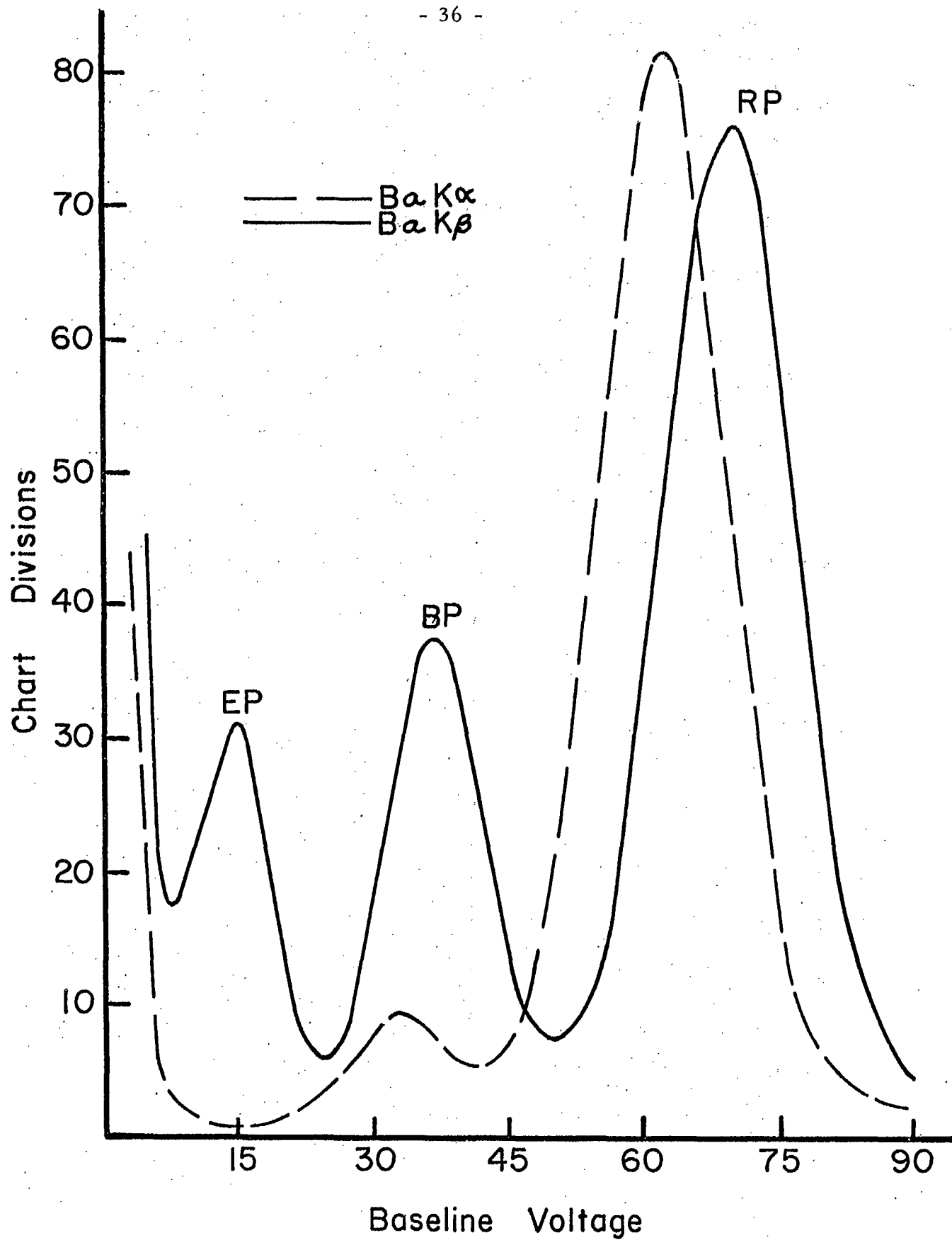


Figure 11. PAD Curves for Second Order Barium Radiation at AG 10 and CV 900.

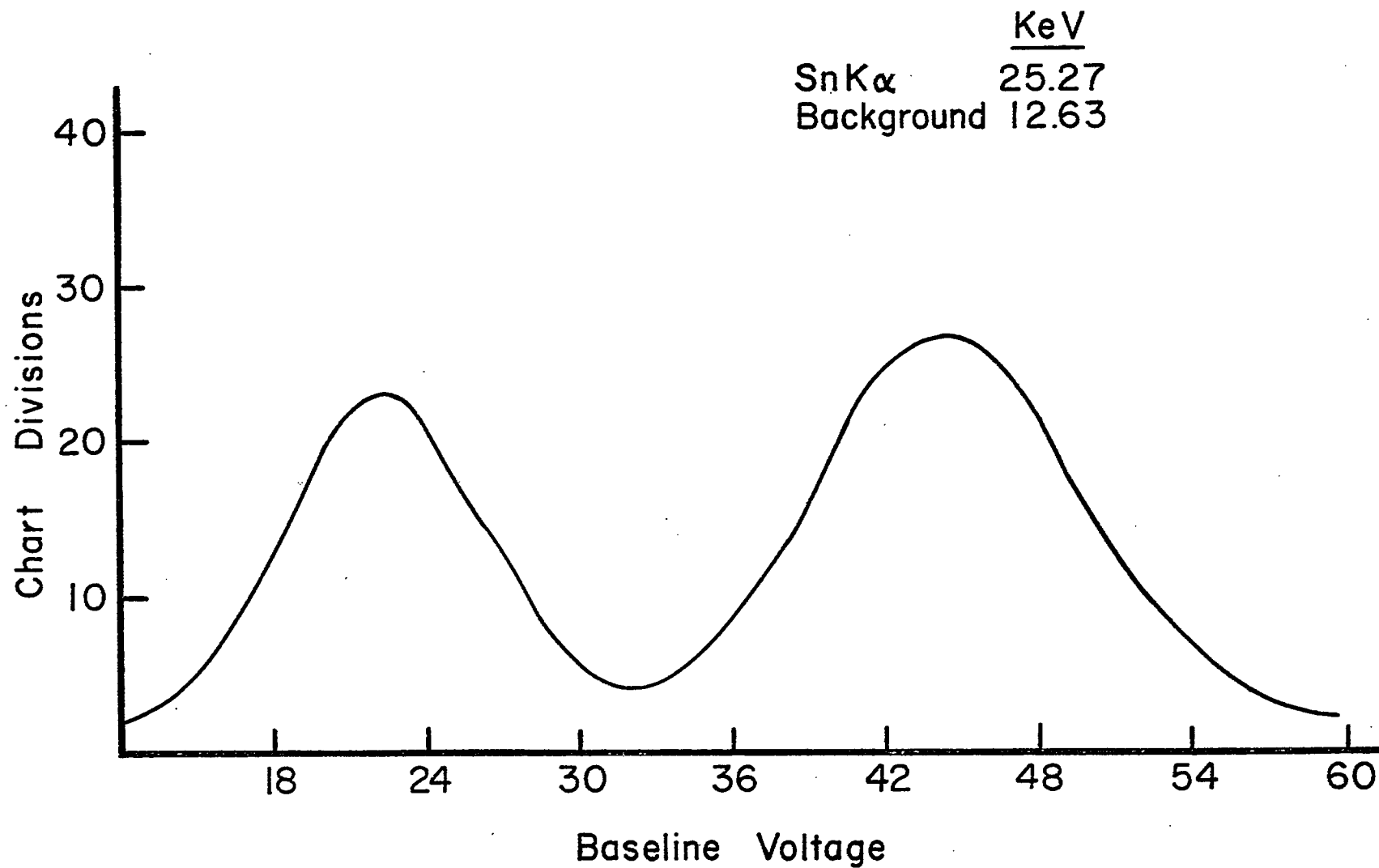


Figure 12. PAD Curves for Second Order SnK $\alpha$  Radiation.

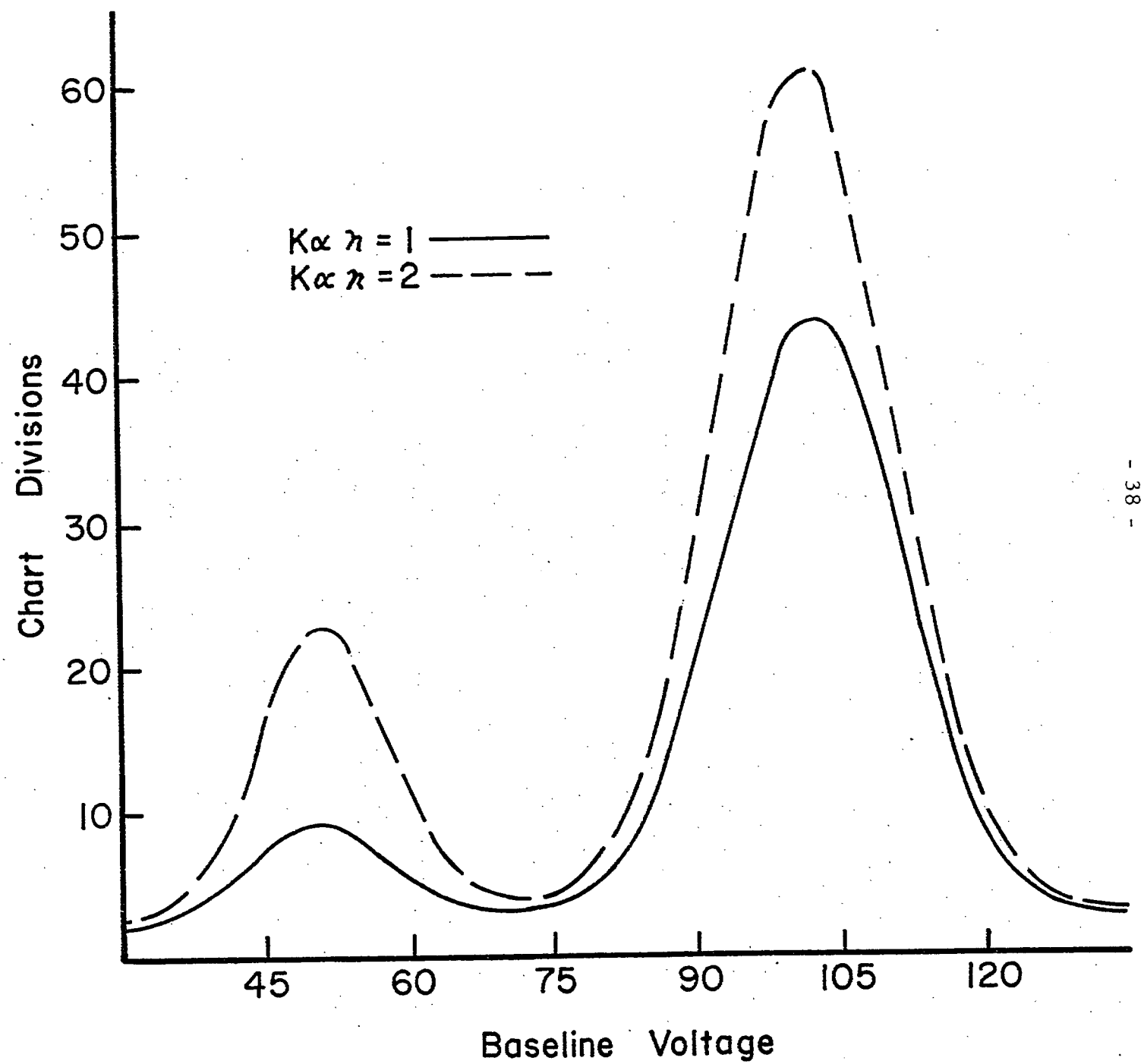


Figure 13. PAD Curves for Hafnium Radiation at AG 10, CV 900.

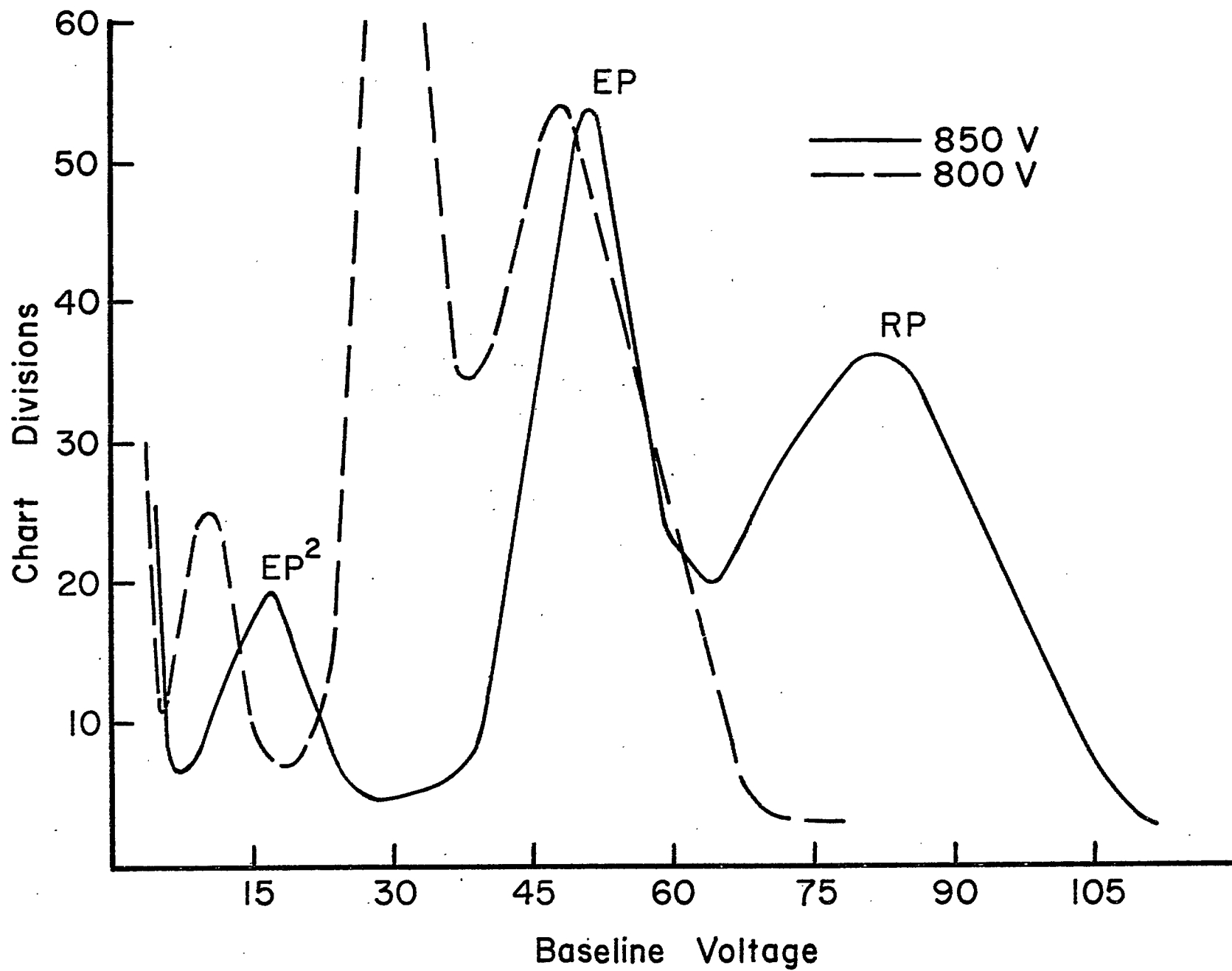


Figure 14. PAD Curves for Second Order  $\text{PbK}\beta_1$  Radiation.

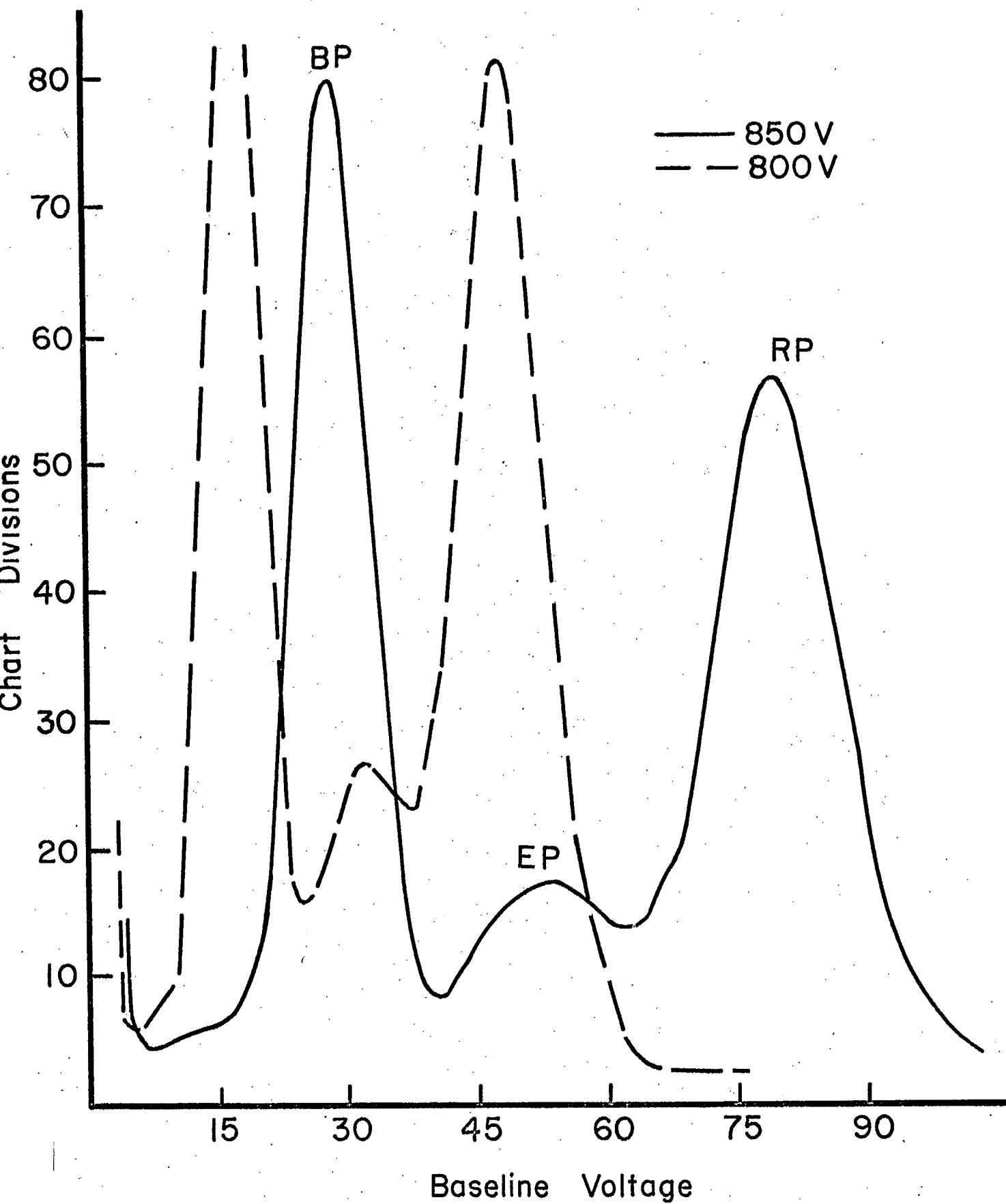


Figure 15. PAD Curves for Third Order HgKa Radiation.

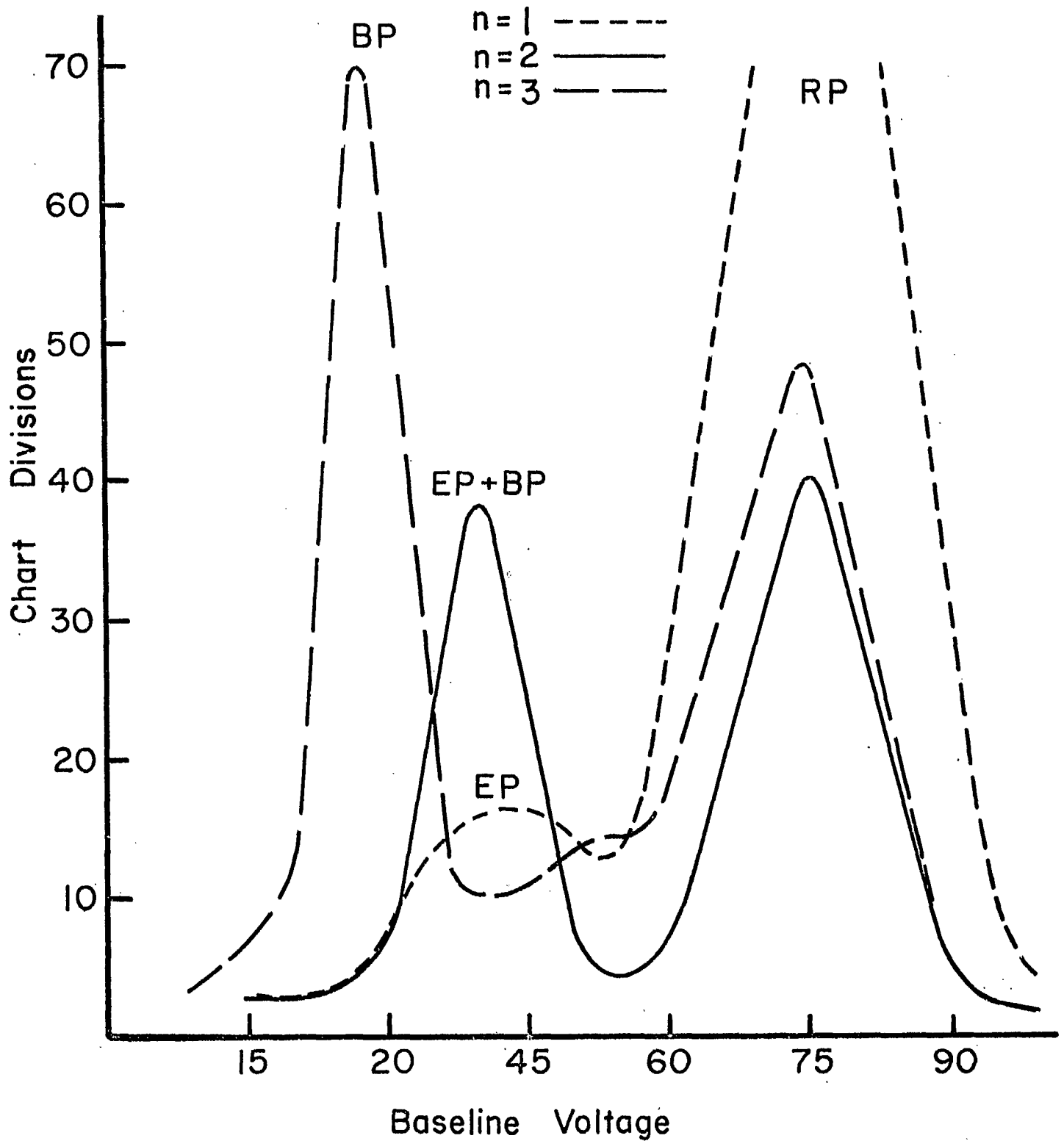


Figure 16. PAD Curves of Hafnium  $K\beta$  Radiation of Different Orders at CV 850.

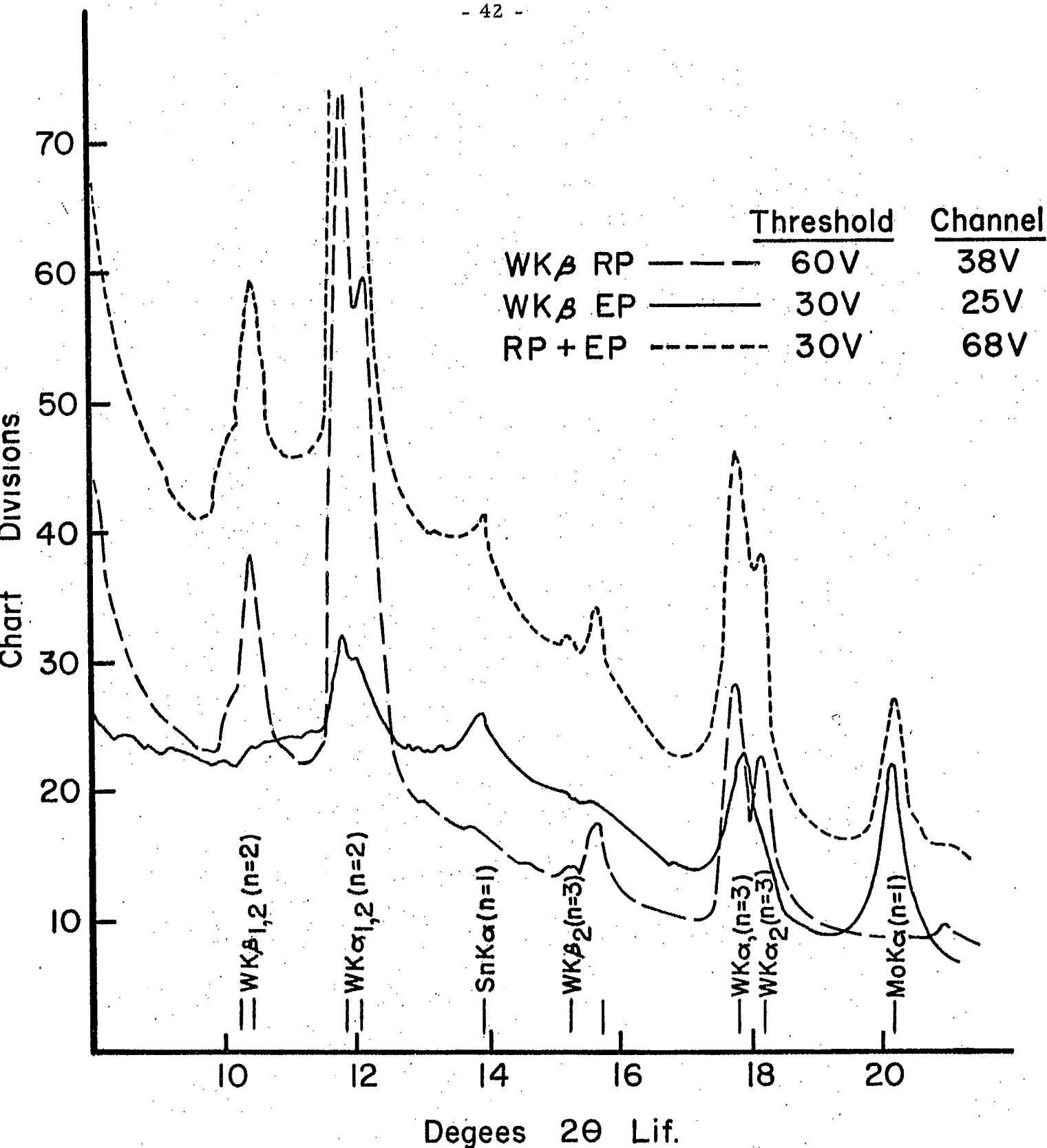


Figure 17. Scans of NBS Standard 841 with and without PHA. 86kV 20mA  
CV 850.